NANO LETTERS

2008
Vol. 8, No. 11
3830-3833

Sub-10 nm Self-Enclosed Self-Limited Nanofluidic Channel Arrays

Qiangfei Xia,[†] Keith J. Morton,[†] Robert H. Austin,[‡] and Stephen Y. Chou*[,†]

NanoStructure Laboratory, Department of Electrical Engineering, Princeton University, Princeton, New Jersey 08544, Department of Physics, Princeton University, Princeton, New Jersey 08544

Received July 22, 2008; Revised Manuscript Received October 2, 2008

ABSTRACT

We report a new method to fabricate self-enclosed optically transparent nanofluidic channel arrays with sub-10 nm channel width over large areas. Our method involves patterning nanoscale Si trenches using nanoimprint lithography (NIL), sealing the trenches into enclosed channels by ultrafast laser pulse melting and shrinking the channel sizes by self-limiting thermal oxidation. We demonstrate that 100 nm wide Si trenches can be sealed and shrunk to 9 nm wide and that λ-phage DNA molecules can be effectively stretched by the channels.

Downloaded by PRINCETON UNIV on September 28, 2009 | http://pubs.acs.org
Publication Date (Web): October 21, 2008 | doi: 10.1021/nl802219b

Extremely narrow enclosed channels are important to fully stretch a single DNA strand for analysis and manipulation.[1,2] Application of semiconductor miniaturization technologies to biophysics has provided, promising tools to make extremely narrow channels to fully stretch a single DNA strand. Previously, electron beam lithography,[3,4] focused ion beam milling techniques,[5] interference lithography,[6] and nanoimprint lithography (NIL)[7−10] have been widely used to pattern nanoscale trenches for this purpose. Among these methods, NIL has particular advantages because it has successfully demonstrated wafer scale fabrication of high density nanofluidic channel arrays with high throughput, low cost, and high resolution.[11−13]

The sealing of nanotrenches into enclosed channels is a critical step in fabrication because leaky channels will destroy the channel operation. A great number of sealing methods have been studied, including sealing with soft elastomers (e.g., polydimethylsiloxane, PDMS),[14] wafer bonding,[15] depositing materials over sacrificial layers (e.g., polycrystalline silicon or polymers) followed by wet etching or thermal decomposition,[16,17] and nonuniform deposition,[7] etc. All the aforementioned methods have their own advantages and disadvantages. For example, PDMS provides a uniform sealing over a large area but the channels might be clogged as soft materials can be easily pressed into the trenches.[12] The wafer bonding technique,[15] on the other hand, provides a rigid seal, but it requires defect free surfaces. Cracks could be introduced when there is a mismatch in the thermal expansion between the substrate and the cover material.

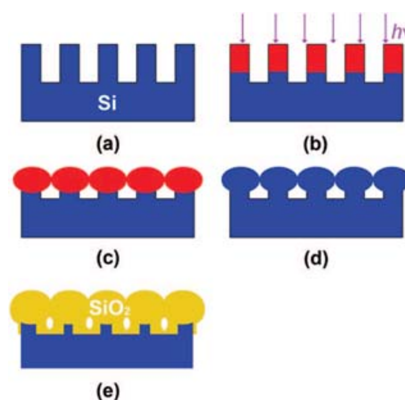

Figure 1. Principle of self-sealing for enclosed nanochannels. (a) Si nanostructures (lines or pillars) made by NIL; (b) a single XeCl laser pulse melts the top layer of the structures; (c) the molten Si flows sideward and joins the neighboring lines (pillars); (d) enclosed channels form after resolidification; (e) channel size shrinking using thermal oxidation.

Here we propose and demonstrate a new method to fabricate enclosed optically transparent nanofluidic channels. The principle of our approach is schematically illustrated in Figure 1. First, Si nanotrenches (either 1D or 2D arrays) are fabricated by NIL and deep reactive ion etching (DRIE) (Figure 1a). These nanostructures are then exposed to an ultraviolet (UV) laser pulse, which melts a thin surface layer of the structures (hundredss of nanometers thick depending on the laser fluence).[18] The melting of Si trenches and pillars can also remove the line edge roughness due to the fact that molten silicon has high surface tension and lower viscosity (the viscosity of molten Si is one-third that of water).[19] The flow of the molten Si layer (Figure 1b) will reshape and seal the trenches (Figure 1c,d). Finally, as an option, a thermal oxidation of Si can further shrink the channel size and make

* Corresponding author. E-mail: chou@princeton.edu.
[†] NanoStructure Laboratory, Department of Electrical Engineering, Princeton University.
[‡] Department of Physics, Princeton University.

10.1021/nl802219b CCC: $40.75 © 2008 American Chemical Society
Published on Web 10/22/2008

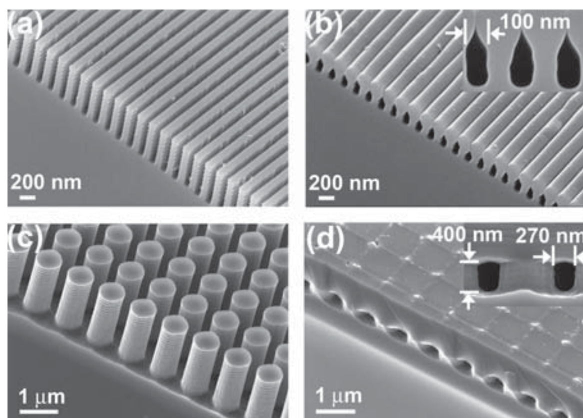

Figure 2. (a) 100 nm wide, 200 nm pitch Si lines (640 nm high). (b) A single laser pulse of 790 mJ/cm^2 turns nanolines in (a) into enclosed Si channels. (c) 700 nm diameter Si pillars (970 nm pitch, 2 μm high) were turned into channels upon exposure to a single laser pulse (d) of 765 mJ/cm^2. Insets in (b) and (d) are zoom in images of the cross section of the nanochannels.

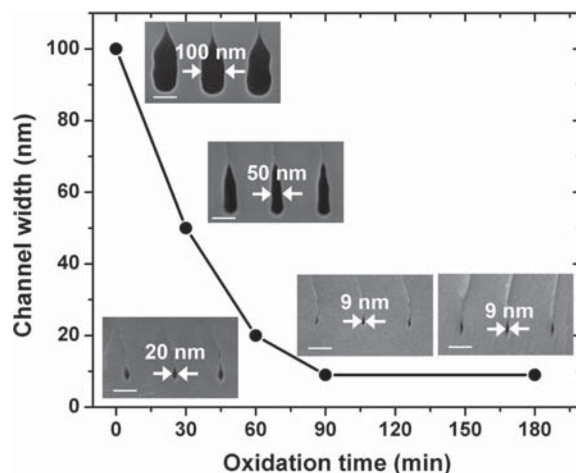

Figure 3. Plot of channel size as a function of wet oxidation time. Insets are the SEM cross sectional images for 100, 50, 20, and 9 nm wide channels, respectively. Note that increasing the oxidation time from 90 to 180 min does not reduce the channel size further.

Downloaded by PRINCETON UNIV on September 28, 2009 | http://pubs.acs.org
Publication Date (Web): October 21, 2008 | doi: 10.1021/nl802219b

the channel optically transparent because Si has become SiO_2 (Figure 1e). The use of NIL inherits NIL's advantages of high patterning precision, high throughput, and low cost. The sealing by a short and material selective UV laser pulse (20 ns) can avoid any melting to the substrate, and the Si oxidation process not only shrinks the channel size to sub-9 nm but also converts the surface layer Si into silicon dioxide, making the channels transparent—a useful feature in DNA detection.

In our experiments we used (100) silicon substrate and patterned trenches with widths of 70 to 270 nm and depths of 640 nm to 2 μm (see Methods for fabrication details). In melting, reshaping, and sealing the Si trenches into enclosed nanochannels, we found that a single laser pulse was sufficient. To optimize the laser melting process, laser fluence was varied from 250 to 1100 mJ/cm^2. For the 100 nm wide/200 nm pitch Si trenches, we found that a laser fluence below 600 mJ/cm^2 did not create enough flow of molten silicon to seal a trench, while a fluence higher than 880 mJ/cm^2 caused partial ablation of the silicon lines. An optimized melting window for the 100 nm wide/200 nm pitch silicon trenches was found to be 690−790 mJ/cm^2.

Figure 2a shows a Si grating structure of 100 nm wide trenches (200 nm pitch, 640 nm depth). After exposure to a single laser pulse of 790 mJ/cm^2, the silicon surface layer melted, flowed, and sealed off to form channels of 100 nm width and 250 nm height (Figure 2b). Similarly, 2D Si pillar arrays (970 nm pitch, 270 nm spacing, 2 μm height) (Figure 2c) were sealed into an interconnected network of 2D channels of 270 nm width and 400 nm height (Figure 2d) upon exposure to a single pulse of 765 mJ/cm^2. We should point out that the rippled top surface of the 1D enclosed channel (Figure 2b) can be improved by using narrower trenches where the molten Si flows a shorter distance. In that case, a self-planarization process of molten Si made the top surface flat (see Supporting Information, Figure S1).

One approach to control the channel size is by varying the laser fluences. Within the processing window, higher laser fluence results in a molten layer that penetrates deeper into the Si surface.[20] As a result, the flow of Si will reshape and seal the trenches to smaller channels. For example, for the starting 2D pillar structure shown in Figure 2c, the channel height became 750 nm after an exposure with a laser pulse of 665 mJ/cm^2 but 400 nm with a laser pulse of 765 mJ/cm^2. This worked for 1D structure as well: for an 1D Si trenches (70 nm wide, 840 nm deep), a laser fluence of 656 mJ/cm^2 created enclosed channels of 450 nm in height and a higher laser fluence of 756 and 857 mJ/cm^2 produced channel heights of 400 and 300 nm, respectively. (See Supporting Information, Figures S2 and S3 for SEM images).

The channel size was further fine-tuned using thermal oxidation because SiO_2 grown from Si has a volume of ~2.4 times larger. The oxidation also made the sealing layer become transparent—a requirement for fluorescence analysis for DNA. The silicon nanochannels sealed by laser melting were put into an oxidation furnace for different lengths of time. Channel widths were measured after 30−180 min of oxidation (Figure 3). The 100 nm wide channels were shrunk to 50, 20, and 9 nm after 30, 60, and 90 min oxidation, respectively. We examined the cross sections at different locations within the sealed area, the channel size was found to be uniform across the laser sealed spot and they were representative as the cleavage points were randomly chosen. Interestingly, we found that increasing the oxidation time above 180 min did not further reduce the channel size, indicating that the oxidation process in this sample was self-limiting.

Although self-limiting oxidation of Si nanowires has been well understood,[21,22] there is little study on the oxidation behavior for the enclosed Si channels. To study this "self-limiting" behavior in Si nanochanels, we delineated the Si and SiO_2 interface of different samples by etching away a small amount of SiO_2 with a diluted HF solution (1:100) for 2.5 min (Figure 4) (note that the channel sizes shown in Figure 4 were a little bit larger than their corresponding ones in Figure 3 due to the HF etch.) As shown in Figure 4a, after 30 min thermal oxidation, there was still a Si core yet

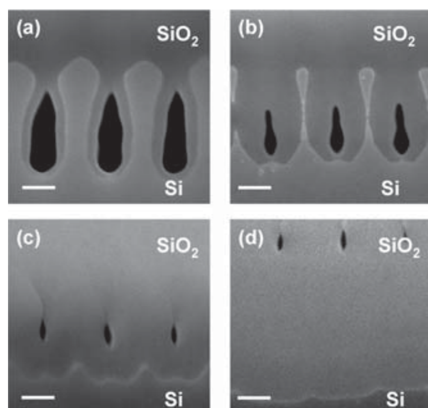

Figure 4. Cross sectional images of laser-sealed channels after oxidation of different durations (a) 30 min; (b) 60 min; (c) 90 min; (d) 180 nm, and 2.5 min diluted HF etch of oxide. The structure before oxidation is shown in the first inset in Figure 3. The SiO_2/Si interfaces are clearly shown after HF dip. Note that the channel sizes were a little bit larger due to the HF etch. Increasing the oxidation time from 90 to 180 min has pushed the SiO_2/Si interface further into the Si bulk. Scale bars: 100 nm.

Downloaded by PRINCETON UNIV on September 28, 2009 | http://pubs.acs.org
Publication Date (Web): October 21, 2008 | doi: 10.1021/nl802219b

to be oxidized between the channels. With the oxidation time increased to 60 min, the Si core size was further reduced while the channel diameter was further shrunk (Figure 4b). The reduction of the channel diameter resulted from the conversion of the Si surrounded a channel into SiO_2. However, as shown in Figure 4c, after 90 min, all Si around the channels (that included the Si between the channels, on the top of the channels, as well as about 100 nm below the channels) was consumed completely to SiO_2. Hence, a further oxidation beyond 90 min did not further reduce the channel diameter but only grew an additional layer of oxide (e.g., ~300 nm for 180 min oxidation) below the channels (Figure 4d). It should be noted that the channel oxidation behavior did depend on the geometry of the starting Si nanostructures. For example, both the capping layer and the duty cycle (channel width/pitch) had played important roles in our study (see Supporting Information, Figures S4 and S5). Further exploration of these parameters will help us design proper starting structures geometry and processes with better control.

We used the oxidized nanochannels to test stretching of λ-phage DNA (48.5 kbp) It is well-known that a DNA molecule forms, in free solution, a random coil configuration with a small radius of gyration (e.g., less than 1 μm for λ-phage DNA),[23,24] but it can be stretched out when physically confined in a nanochannel that is much smaller than this radius of gyration and on the order of the polymer's persistence length,[25] which is approximately 50 nm for double-stranded DNA in typical buffers.[9] We tested the stretch of λ-phage DNA, suspended in a buffer solution (0.5 $\times$ TBE), into the 20 nm wide, 60 nm tall nanochannels fabricated by self-sealing and oxidation (Figure 3, 1 h oxidation). The channels were prewetted (see Methods for details). Figure 5 is a typical optical image showing several individual DNA molecules and DNA fragments stretched and aligned in the parallel nanochannels. Over 50 elongated DNA pieces were analyzed. The lengths of the 10 longest molecules were measured to be between 11 and 13 μm or 60−70% of the 18.5 μm dye-adjusted total contour length.

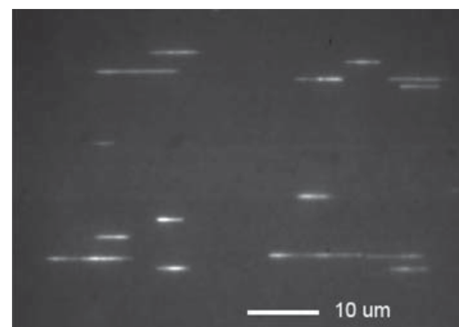

Figure 5. CCD image of λ-phage DNA stretched in 20 nm wide nanochannels that were self-sealed and underwent 1 h thermal oxidation. The DNA molecules have been effectively stretched.

Even though the sealed and oxidized nanochannels have an elliptical shape, these results are consistent with previous theoretical and experimental results for λ-phage DNA at this ionic strength.[9]

The flow and stretching of the molecules in the channels verifies the continuity of the enclosed channels. The continue flow of DNA also suggests the fabrication process generates uniform channel width, as a nonuniform channel width fabrication process would have closed certain parts of the channel.

The laser sealing process can be applied for complicated biodevices, for example, by adjusting the laser spot size and controlling the laser sport position, we can expose certain specific areas needed to be sealed while leaving other areas untouched. This flexibility is necessary for complicated biochips that have different functional devices on one chip. The self-sealing process does not involve complicated equipments and processes. It does not require extra process and material to seal the trenches, neither does it require exceptionally flat surfaces for sealing. These make our method simple in operation and economical in production.

Finally, the principle of our method can be extended to channels made from other materials using lasers of different wavelengths. For example, a CO_2 laser can be used for SiO_2 channels because SiO_2 can be melted by absorbing the laser pulse in this wavelength range.[26,27]

In summary, we have proposed and demonstrated a simple method for sealing, reshaping, and shrinking NIL patterned nanostructures into nanofluidic channels. Using a single laser pulse, 1D and 2D silicon nanochannels were self-sealed, with channel size controlled by laser fluence. Thermal oxidation was used to fine-tune the channel size to sub-10-nm regime. We discovered that this oxidation process is self-limiting for the enclosed silicon channels. As an ultrafast, material selective process, our approach is simple in operation and economical in production. It has demonstrated to be suitable for applications in DNA stretching and promising for other laboratory-on-a chip devices.

Methods. Fabrication of Si Nanotrenches. Si nanostructures were fabricated by DRIE using NIL patterned thermal oxide as an etching mask. Fabrication of nanoscale trench and pillar arrays started with p-type (100) silicon wafers capped with 30 nm thick thermal oxide. After cleaning in a solution (NH_4OH:H_2O_2:deionized H_2O = 1:1:5) at 80 °C for

15 min (RCA no. 1), the wafers were first spin coated with a 180 nm thick thermoplastic imprint resist (NXR 1020, Nanonex Corp, NJ), followed by baking on a hot plate at 70 °C for 15 min to drive out the residual solvent. Silicon master molds (made by interference lithography and RIE) having parallel lines of 200 nm pitch or pillars of 970 nm pitch over 4 in. wafers were used to imprint the resist. The patterns on the imprinted resists were then transferred to the thermal oxide layers by RIE in a Plasmatherm SLR 720 RIE system (Plasmatherm, St. Petersburg, FL) using a CHF_3/O_2 chemistry, with 10 sccm CHF_3, 1.5 sccm O_2, 5 mTorr base pressure, and 70 mW/cm^2 power density. The patterned thermal SiO_2 was then served as a hard mask for silicon etching using deep RIE (STS, Newport, UK). The Si etching had several cycles depending on the depth wanted. Each cycle started with an etch step (30 sccm SF_6, 6 sccm O_2, 600 W ICP power, 15 W platen power, 15 mTorr base pressure, 7 s), followed by a passivatation step (85 sccm C_4F_8, 600 W ICP power, 15 mTorr base pressure, 5 s). The etched samples (trenches of 200 nm pitch and pillars of 970 nm pitch) were dipped into diluted HF to strip the SiO_2 mask, followed by a further cleaning using RCA no. 1 for 15 min.

Laser Melting and Thermal Oxidation. The fabricated structures were then exposed to a XeCl excimer laser (Compex Pro102, Lambda Physik, Germany) with a wavelength of 308 nm, pulse duration of 20 ns, and spot size of 3 × 3 mm^2. In each case, a single laser pulse with an appropriate fluence was used to just melt the top of the structures, resulting in enough melting and a uniform sealing over the exposed area. The molten time (the duration during which the surface is liquid) can be measured using a time-resolved reflectivity technique as metal-like liquid silicon has higher reflectivity than solid Si.[18,20] Using this method, we measured the molten time for Si as a function of laser fluence. For a laser pulse of 765 mJ/cm^2, the molten time is about 60 ns. Because a full sealing is completed while the silicon is in a liquid state, the estimated flow speed of the molten silicon in this case is about 2 m/s (see Supporting Information, Figure S6).

Some channel samples were then put into a Tystar oxidation tube (Tystar Corp, CA) for a standard wet thermal oxidation process at 1000 °C. After oxidation, the samples were cleaved 1 mm away from the edge of the sealed area and perpendicular to the channels to expose the channel openings for SEM imaging and DNA stretching experiments.

DNA Stretching. For the DNA stretching experiments, λ phage DNA (48.5 kbp, New England BioLabs) at a concentration of 1 μg/mL in 0.5× TBE buffer (0.045 M tris-base, 1 mM EDTA with 0.045 M boric acid) were loaded into the channels by capillary action. The DNA was labeled with TOTO-1 (Molecular Probes, 1 dye molecule per 10 bp) and imaged using a Pentamax ICCD camera (Roper Scientific, NJ) on a Nikon Eclipse TE2000 fluorescence microscope (488 nm excitation/514 nm emission) with a Nikon 100× oil immersion objective (NA = 1.4).

Downloaded by PRINCETON UNIV on September 28, 2009 | http://pubs.acs.org
Publication Date (Web): October 21, 2008 | doi: 10.1021/nl802219b

Acknowledgment. We thank U.S. Defense Advanced Research Program Agency (DARPA), Office of Naval Research (ONR), for their partial financial support to the project.

Supporting Information Available: Information about the top surface roughness after laser sealing, laser fluence dependence of channel height, geometry dependence of channel oxidation, and Si molten time as a function of laser fluence. This material is available free of charge via the Internet at http://pubs.acs.org.

References

(1) Austin, R. H.; Brody, J. P.; Cox, E. C.; Duke, T.; Volkmuth, W. *Phys. Today* **1997**, *50*, 32–38.
(2) Austin, R. H.; Tegenfeldt, J. O.; Cao, H.; Chou, S. Y.; Cox, E. C. *IEEE Trans. Nanotechnol.* **2002**, *1*, 12–18.
(3) Harnett, C. K.; Coates, G. W.; Craighead, H. G. *J. Vac. Sci. Technol., B* **2001**, *19*, 2842–2845.
(4) Asoh, H.; Nishio, K.; Nakao, M.; Yokoo, A.; Tamamura, T.; Masuda, H. *J. Vac. Sci. Technol., B* **2001**, *19*, 569–572.
(5) Cannon, D. M.; Flachsbart, B. R.; Shannon, M. A.; Sweedler, J. V.; Bohn, P. W. *Appl. Phys. Lett.* **2004**, *85*, 1241–1243.
(6) O'Brien, M. J., II; Bisong, P.; Ista, L. K.; Rabinovich, E. M. *J. Vac. Sci Technol., B* **2003**, *21*, 2941–2945.
(7) Cao, H.; Yu, Z.; Wang, J.; Tegenfeldt, J. O.; Austin, R. H. *Appl. Phys. Lett.* **2002**, *81*, 174–176.
(8) Guo, L. J.; Cheng, X.; Chou, C. F. *Nano Lett.* **2004**, *4*, 69–73.
(9) Reisner, W.; Morton, K. J.; Riehn, R.; Wang, Y. M.; Yu, Z.; Rosen, M.; Sturm, J. C.; Chou, S. Y.; Frey, E.; Austin, R. H. *Phys. Rev. Lett.* **2005**, *94*, 196101.
(10) Liang, X.; Morton, K. J.; Austin, R. H.; Chou, S. Y. *Nano Lett.* **2007**, *7*, 3774–3780.
(11) Chou, S. Y.; Krauss, P. R.; Renstrom, P. J. *Appl. Phys. Lett.* **1995**, *67*, 3114–3116.
(12) Chou, S. Y.; Krauss, P. R.; Renstrom, P. J. *Science* **1996**, *272*, 85–87.
(13) Chou, S. Y.; Krauss, P. R.; Zhang, W.; Guo, L. J.; Zhuang, L. *J. Vac. Sci. Technol., B* **1997**, *15*, 2897–2904.
(14) Chou, H. P.; Spence, C.; Scherer, A.; Quake, S. *Proc. Natl. Acad. Sci. U.S.A.* **1999**, *96*, 11–13.
(15) Stjernstrom, M.; Roeraade, J. *J. Micromech. Microeng.* **1998**, *8*, 33–38.
(16) Li, W. L.; Tegenfeldt, J. O.; Chen, L.; Austin, R. H.; Chou, S. Y.; Kohl, P. A.; Krotine, J.; Sturm, J. C. *Nanotechnology* **2003**, *14*, 578–583.
(17) Turner, S. W.; Perez, A. M.; Lopez, A.; Craighead, H. G. *J. Vac. Sci. Technol., B* **1998**, *16*, 3835–3840.
(18) Chou, S. Y.; Keimel, C.; Gu, J. *Nature* **2002**, *417*, 835–837.
(19) Chou, S. Y.; Xia, Q. F. *Nat. Nanotechnol.* **2008**, *3*, 295–300.
(20) Auston, D. H.; Golovchenko, J. A.; Simons, A. L.; Surko, C. M.; Venkatesan, T. N. C. *Appl. Phys. Lett.* **1979**, *34*, 777–779.
(21) Liu, H. I.; Biegelsen, D. K.; Johnson, N. M.; Ponce, F. A.; Pease, R. F. W. *J. Vac. Sci. Technol., B* **1993**, *11*, 2532–2537.
(22) Liu, H. I.; Biegelsen, D. K.; Ponce, F. A.; Johnson, N. M.; Pease, R. F. W. *Appl. Phys. Lett.* **1994**, *64*, 1383–1385.
(23) Smith, D. E.; Perkins, T. T.; Chu, S. *Macromolecules* **1996**, *29*, 1372–1373.
(24) Stein, D.; van der Heyden, F. H. J.; Koopmans, W. J. A.; Dekker, C. *Proc. Natl. Acad. Sci. U.S.A.* **2006**, *103*, 15853–15858.
(25) Tegenfeldt, J. O.; Prinz, C.; Cao, H.; Chou, S.; Reisner, W. W.; Riehn, R.; Wang, Y. M.; Cox, E. C.; Sturm, J. C.; Silberzan, P.; Austin, R. H. *Proc. Natl. Acad. Sci. U.S.A.* **2004**, *101*, 10979–10983.
(26) McLachlan, A. D.; Meyer, F. P. *Appl. Opt.* **1987**, *26*, 1728–1731.
(27) Armani, D. K.; Kippenberg, T. J.; Spillane, S. M.; Vahala, K. J. *Nature* **2003**, *421*, 925–928.

NL802219B